Dynamic Error Measure for Curve Scan-Conversion

Xiaolin Wu
Department of Mathematical Sciences
University of Lethbridge
Lethbridge, Alta. Canada T1K 3M4

Jon Rokne
Department of Computer Science
University of Calgary
Calgary, Alta. Canada T2N 1N4

March 1989

Abstract–This paper reports some pioneering results on a new research topic in computer graphics: the measurement of raster image quality in terms of reproduction of curve spatial coherence when it has been generated by scan-conversion. A dynamic error for curve scan-conversion is defined to measure the distortion of curve spatial coherence (the dynamic context, smoothness and continuity of the original curve) caused by scan-conversion. It is shown that the previous criterion of minimizing the distance between the pixel chosen and the actual curve may fail to reproduce the most aesthetic discrete curves allowed by a given resolution. Analytic results are given to argue that the new dynamic error measure is superior to the previous measure for overall raster image quality.

Key words: Curve scan-conversion, anti-aliasing, error analysis, realism, vector and matrix norms,

1 Introduction

A 2-dimensional continuous curve is usually associated with an implicit function $f(x,y) = 0$. This relation between geometry and algebra can be intuitively understood by viewing the curve as the locus of a moving point in the Euclidean plane where the motion is restricted by the function $f(x,y) = 0$. At any moment t the coordinates of the moving point are (x_t, y_t) such that $f(x_t, y_t) = 0$. There are two kinds of information contained in a continuous curve of a function $f(x,y) = 0$ from this perspective:

- the static position of the curve after the point finishes its movement, i.e., the curve coordinates (x_t, y_t) for all t;

- the dynamic displacement of the point while it is moving, i.e., the relation between coordinates (x_t, y_t) and $(x_{t+\Delta t}, y_{t+\Delta t})$.

These two kinds of information are called the static and the dynamic information of the curve $f(x,y) = 0$. The dynamic information (which we focus on here) reflects the spatial coherence among parts of the curve, or the *dynamic context* of the curve as referred to in the sequel.

In order to draw the curve $f(x,y) = 0$ on raster devices, a process known as scan-conversion in computer graphics is used to approximate the curve $f(x,y) = 0$ with a finite number of lattice points (pixels). This set of pixels is called a *discrete image* of the original curve. For a good reproduction of a continuous curve in a finite lattice (raster plane), the scan-conversion process should retain both the static and dynamic information of the original curve to the maximum precision. If the static information of a continuous curve could be exactly rendered on rasters, then the dynamic information of the curve would be also retained without error. This is unfortunately impossible due to finite precision of the raster plane. No matter what scan-conversion scheme is used, the majority of the pixels it chooses will deviate from the original curve. Consequently, the displacement of a pair of points on the continuous curve will be distorted by the scan-conversion as well.

In many applications of computer graphics, the major criterion for plotting a continuous curve on raster devices is whether or not it appeals to the viewer, where the preservation of the dynamic information of the original curve is of primary concern. In terms of human perception of geometric figures, our eyes are more sensitive to the dynamic context of a figure than they are to its absolute spatial position. A viewer may not realize that an entire object on a display medium has been translated if the amount of the shift is relatively small compared with the size of the background or if the background is blank with no refrerence point to the object. He will, however, easily catch a slight distortion of the dynamic context of the object as an unpleasant alias (jaggy). The task of anti-aliasing in computer graphics

may therefore be considered to be the minimization of the loss of dynamic information from an original curve due to scan-conversion.

Clearly, analyzing the performances of scan-conversion schemes in terms of rendering the dynamic information of an original curve on rasters, is of both theoretical and practical importance. Unfortunately, to our knowledge, no research explicitly aiming at this topic has been done so far. Up to now quite a lot of quantitative measures have been used for measuring the errors in scan-converting a continuous curve on rasters and some results about the performance of a scan-conversion scheme on general or some particular curves have been reported [3,4,6,7,8,9,10,12,13]. All these previous measures should be, however, classified as static measures, because they essentially treat errors as geometric distances between the original curve and its discrete image in various norms. In other words these measures emphasize the absolute errors between the static positions of an original curve and its discrete image.

The major objective of this paper is to propose a dynamic error measure that will assess the distortion of the dynamic context of an original curve by scan-conversion. A theoretic analysis is also conducted on the capability of the well-known Bresenham's curve scan-conversion scheme to render the dynamic information of the original curves under the new measure. The results of our analysis shows that the new measure represents the distortion of curve caused by the scan-conversion realistically. It is also shown that the dynamic error measure is objective and informative, that is, assesses the image quality of discrete curves well.

The following section provides the necessary preliminaries and it defines the dynamic error for curve scan-conversion. In section 3 the paper proceeds to compute the bounds of the dynamic errors associated with the Bresenham's curve scan-conversion scheme. It is shown that the current curve scan-conversion algorithms which are optimal under static error measures do not necessarily perform well under the dynamic error measure. More detailed studies of the performance of Bresenham's scan-conversion scheme under the dynamic error measure are conducted on lines in section 4 and then on general convex curves in section 5. The paper concludes with a brief mention of the continuing research on the topic.

2 Preliminaries

It is the convention of this paper that variables in capital style are integer and variables in lower case or greek letters are real except for small letters from i to n which also des-

ignate integers. The symbols $\mathcal{R}$ and $\mathcal{Z}$ stand for the set of all real numbers and the set of all integers.

A general continuous 2-dimensional curve $f(x,y) = 0$ is expressed by the explicit function $y = g(x)$ such that $f(x, g(x)) = 0$, for easy algebraic manipulation later. The scan-conversion of $g(x)$ from the Euclidean plane onto the raster plane is a many-to-one map $\mathcal{F} : \mathcal{R}^2 \to \mathcal{Z}^2$. The image of a bounded curve $g(x)$ under the map $\mathcal{F}$, denoted by $\mathcal{F}[g(x)]$, may be viewed as a finite set of lattice points, or as an n-tuple $\mathcal{F}[g(x)] = \langle(X_i, Y_i)\rangle$, $(X_i, Y_i) \in \mathcal{Z}^2$, $1 \le i \le n$. An $\mathcal{F}[g(x)]$ is called an 8-connected discrete curve if

$$[(X_{i+1} - X_i)^2 + (Y_{i+1} - Y_i)^2]^{\frac{1}{2}} \le \sqrt{2}, \quad 1 \le i < n, \quad (1)$$

and a 4-connected curve if

$$[(X_{i+1} - X_i)^2 + (Y_{i+1} - Y_i)^2]^{\frac{1}{2}} = 1, \quad 1 \le i < n. \quad (2)$$

In practice, two types of $\mathcal{F}$, called the diamond scheme and the square scheme, denoted separately by $\mathcal{F}_\diamond$ and $\mathcal{F}_\square$, are commonly used. Their geometric interpretations are given in Figure 1 which shows that $(X_i, Y_i) \in \mathcal{F}_\diamond[g(x)]$ or $(X_i, Y_i) \in \mathcal{F}_\square[g(x)]$ if and only if the curve $g(x)$ enters the the diamond, or the square region centered at (X_i, Y_i). Under L_p-metric (Minkowski metric), the L_p-distance between two points (x_0, y_0) and (x_1, y_1) is defined by

$$(|x_1 - x_0|^p + |y_1 - y_0|^p)^{1/p} \quad (3)$$

then the diamond in Figure 1(a) is the half unit ball for the L_1-metric in the sense that all its boundary points have 1/2 L_1-distance from its center. Similarly, the square in Figure
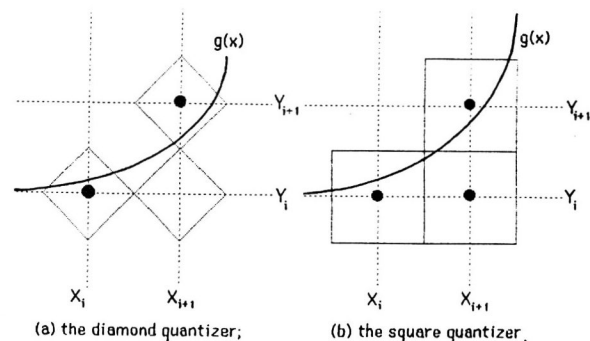

(a) the diamond quantizer;   (b) the square quantizer.

Figure 1: Two different quantizers

1(b) is the half unit ball in terms of the L_∞-distance. The scheme $\mathcal{F}_\diamond$ was first adopted by Bresenham [2] (the so called Bresenham's scheme in the sequel) and since then various implementations of this scheme for plotting different curves have appeared in the literature [1,5,6,13]. Clearly, under the usual definition of discrete curve [11, p.152], $\mathcal{F}_\diamond[g(x)]$ is an 8-connected discrete curve provided $g(x)$ is continuous.

The scheme $\mathcal{F}_\square$ was used [6,13] to generate 4-connected discrete images from continuous curves.

Since our goal is to find a measurement for the smoothness of the discrete images of the continuous curves being scan-converted, we consider the class of twice differentiable functions which includes all common graphics primitives. Then $y = g(x)$ can be partitioned into segments such that on each of these segments $g'(x)$ falls into one of four ranges $(-\infty, -1]$, $(-1, 0]$, $(0, 1]$, $[1, \infty)$ and $g''(x)$ falls into either of two ranges $(-\infty, 0]$, $[0, \infty)$. These curve segments whose 1st and 2nd derivatives are bounded as above are called *octant segment*. Over all the combinations of the four ranges for $g'(x)$ and the two for $g''(x)$ there are eight different octant segments. Because of the symmetry among the eight different octant segments, it is sufficient to consider one of them. Therefore, unless stated otherwise, the studies of the curve $g(x)$ hereafter will be restricted to its particular octant segment where $0 \leq g'(x) \leq 1$ and $g''(x) \geq 0$. The generalization to the other seven octant segments of $g(x)$ is straightforward. For this chosen octant segment of the curve $g(x)$ the scan-conversion is normally propagated along the x axis one raster unit at a time, assuming that $g(x)$ has been scaled according to the resolution of the raster display. At the ith step of the process, the point on the curve $(X_i, g(X_i))$, $X_i = X_{i-1} + 1$, is sampled and then approximated by the pixel (X_i, Y_i) for a chosen Y_i. Therefore, we would like to measure the error in scan-conversion with respect to the y coordinates.

If $(X_i, Y_i) \in \mathcal{F}[g(x)]$, then the *linear error* in y at the pixel (X_i, Y_i), denoted by E_i, is defined by

$$E_i \equiv g(X_i) - Y_i. \tag{4}$$

Consider another pixel $(X_j, Y_j) \in \mathcal{F}[g(x)]$ and let

$$y_{i,j} \equiv g(X_j) - g(X_i),$$
$$Y_{i,j} \equiv Y_j - Y_i. \tag{5}$$

The *dynamic error* in y and with i and j as parameters, denoted by $\mathcal{E}_{i,j}$, is defined by the expression

$$\mathcal{E}_{i,j} \equiv \begin{cases} 0 & \text{if } i = j \\ \frac{y_{i,j} - Y_{i,j}}{j - i} & \text{if } i \neq j \end{cases}, \quad 1 \leq i, j \leq n, \tag{6}$$

which is simply a relative error in y displacement over the sample distance of the two pixels in question. In particular, $\mathcal{E}_{i,i+1}$ $(1 \leq i < n)$ is called the *unit dynamic error* and denoted by e_i. By (5) and (6), any $\mathcal{E}_{i,j}$ $(i \neq j)$ is a linear combination of unit dynamic errors such that

$$\mathcal{E}_{i,j} = \frac{1}{j - i} \sum_{k=i}^{j-1} e_k. \tag{7}$$

Also by the definition (6) the relation between the dynamic error and the linear error,

$$\mathcal{E}_{i,j} = \frac{E_j - E_i}{j - i}, \tag{8}$$

is immediate.

Given a curve $g(x)$ and a scan-conversion operator $\mathcal{F}$, global measurements are needed to evaluate the overall quality of $\mathcal{F}[g(x)]$. Let $\mathbf{d}$ denote an error vector $\langle E_i \rangle$ or $\langle e_i \rangle$, then a vector norm $\|\mathbf{d}\|$ will naturally serve the purpose. In this paper the two norms : the 1-norm

$$\|\mathbf{d}\|_1 = \sum_{i=1}^{n} |d_i| \tag{9}$$

and the ∞-norm

$$\|\mathbf{d}\|_\infty = \max_{1 \leq i \leq n} |d_i| \tag{10}$$

are used.

The set of dynamic errors $\mathcal{E}_{i,j}$ on a discrete curve $\mathcal{F}[g(x)]$, where $1 \leq i, j \leq n$ and n is the cardinality of $\mathcal{F}[g(x)]$, constitute an $n \times n$ matrix $\{\mathcal{E}_{i,j}\}$. Thus a matrix norm of some kind will be useful for analysing the dynamic errors. In addition to the conventional matrix ∞-norm [1]

$$\|\mathcal{E}\|_\infty = \max_{1 \leq j \leq n} \sum_{i=1}^{n} |\mathcal{E}_{i,j}|, \tag{11}$$

we found in our experiments that another matrix norm defined by

$$\|\mathcal{E}\|_* = \sum_{i=1}^{n} \sum_{j=1}^{n} |\mathcal{E}_{i,j}| \tag{12}$$

is more objective as a global measure for distortion of curve dynamic context by scan-conversion. It is easy to show that for any two $n \times n$ matrices $\mathbf{A}$ and $\mathbf{B}$

$$\|\mathbf{A}\|_* = 0 \text{ if and only if } \mathbf{A} = \mathbf{0}$$
$$\|\alpha\mathbf{A}\|_* = \|\alpha\| \cdot \|\mathbf{A}\|_*, \quad \alpha \in R$$
$$\|\mathbf{A} + \mathbf{B}\|_* \leq \|\mathbf{A}\|_* + \|\mathbf{B}\|_* \tag{13}$$

hold, verifying that (12) indeed defines a matrix norm as given by the above axioms. Only the multiplicative property (not needed here) does not hold.

3 Dynamic Error Analysis

Given a curve $g(x)$ the dynamic errors on $\mathcal{F}[g(x)]$ differ from one scan-conversion scheme to another. The most popular is Bresenham's scheme $\mathcal{F}_\circ$, hence much of the attention of this paper will be given to this scheme. Suppose

---

[1] Since the matrix $\{\mathcal{E}_{i,j}\}$ is symmetric, its ∞-norm and 1-norm are identical.

that $(X_i, Y_i), (X_j, Y_j) \in \mathcal{F}_\circ[g(x)]$, $1 \leq i, j \leq n$. Then for the chosen octant segment of $g(x)$ where $0 \leq g'(x) \leq 1$, we have

$$Y_i = \lfloor g(X_i) + 1/2 \rfloor, \tag{14}$$

based on the observation of Figure 1 (a). By subjecting the floor function to the inequalities

$$\alpha - 1/2 < \lfloor \alpha + 1/2 \rfloor \leq \alpha + 1/2, \quad \alpha \in \mathcal{R}, \tag{15}$$

the bound for the static line errors

$$-1/2 < E_i \leq 1/2 \tag{16}$$

is obtained. Since E_i is defined as the distance between a real number and an integer, the value $1/2$ is the greatest lower bound to $\|\mathbf{E}\|_\infty$, i.e., the diamond quantizer $\mathcal{F}_\circ$ minimizes $\|\mathbf{E}\|_\infty$. It is also trivially true that the scheme $\mathcal{F}_\circ$ minimizes $\|\mathbf{E}\|_1$ as well. So Bresenham's scheme is already 'optimal' if the rendering of the static curve position is the sole criterion for curve scan-conversion.

As argued in introduction, however, it is more desirable to minimize $\|\mathcal{E}\|$ for aesthetic visual effect, that is, to restrain the magnitude of the dynamic errors. Now consider the dynamic errors associated with Bresenham's scheme. Noting that

$$Y_{i,j} = \lfloor g(X_j) + 1/2 \rfloor - \lfloor g(X_i) + 1/2 \rfloor \tag{17}$$

for any $(X_i, Y_i), (X_j, Y_j) \in \mathcal{F}_\circ[g(x)]$ and applying (15) to the right side of (17), we obtain

$$-1 < y_{i,j} - Y_{i,j} < 1. \tag{18}$$

From the definition of dynamic error (6) the bound $|\mathcal{E}_{i,j}| < 1$ follows immediately. Indeed, -1 and 1 are the greatest lower bound and the smallest upper bound for $\mathcal{E}_{i,j}$ associated with the scheme $\mathcal{F}_\circ$. Consider the case where $g(X_{i+1}) = Y' + 1/2 - \epsilon$ and $g(X_i) = Y' - 1/2$ for some infinitesimal $\epsilon > 0$. Then $Y_{i,i+1} = 0$ by (17) hence $\lim_{\epsilon \to 0} e_i = 1$ by (6); similarly, if $g(X_{i+1}) = Y' - 1/2$, $g(X_i) = Y' - 1/2 - \epsilon$ with some infinitesimal $\epsilon > 0$, then $\lim_{\epsilon \to 0} e_i = -1$.

If there is no constraint of choosing $Y_{i,j}$ as (17) required by $\mathcal{F}_\circ$, however, then it is possible to choose $Y_{i,j}$ for any given X_i and X_j such that $\max_{i,j}\{|\mathcal{E}_{i,j}|\} < 1/2$, simply because $\mathcal{E}_{i,j}$ is a difference between the real value $y_{i,j}$ and the integer $Y_{i,j}$. This suggests that the scheme $\mathcal{F}_\circ$ may fail to minimize $\|\mathcal{E}\|$. For example, consider the geometry of Figure 2 where the three pixels indicated by solid dots are chosen by $\mathcal{F}_\circ$ as the discrete image of the continuous curve segment. If, however, the pixel labeled by o replaces the one just above it, then the magnitude of the particular e_i is minimized. Visually, the new pixel layout after the above

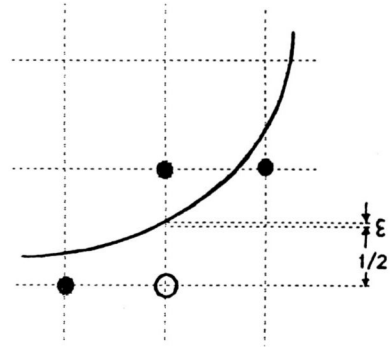change does give a much better representation of the dynamic context of the original curve segment. Note that the

Figure 2: A case where $\mathcal{F}_\circ$ fails to minimize the dynamic error.

original convex curve segment in question is mapped by $\mathcal{F}_\circ$ to a concave pixel pattern. By choosing the pixel marked by o we correct this error in convexity. Unfortunately, the criterion of minimizing $\|\mathcal{E}\|$ often conflicts against that of minimizing $\|\mathbf{E}\|$. As illustrated by Figure 2 if the pixel labeled by o is chosen then $|E_i| = 1/2 + \epsilon$, otherwise there would be $|E_i| < 1/2$.

On the other hand, the inequalities (18) imply that the integer $Y_{i,j}$ can be only one of two possible values: $\lfloor y_{i,j} \rfloor$ or $\lceil y_{i,j} \rceil$ over all $1 \leq i, j \leq n$. Therefore, $|\mathcal{E}_{i,j}|$ generally gets smaller as $|j - i|$ increases. It is easy to see that

$$\|\mathbf{e}\|_\infty = \max_{i,j}\{|\mathcal{E}_{i,j}|\}. \tag{19}$$

This means that the scheme $\mathcal{F}_\circ$ will not seriously distort the overall curvature of curves of sufficient length. That is why a discrete circle may macroscopically look very much like a circle even though microscopically its segments do not look like circular arcs at all having unpleasant jaggies.

It is therefore desirable to evaluate the value of $\|\mathcal{E}\|$ in order to study the overall image quality. Unfortunately, given a curve $g(x)$, a closed form for $\|\mathcal{E}\|$ is difficult to obtain. The complication of deriving $\|\mathcal{E}\|$ directly can be avoided by computing the vector norm $\|\mathbf{e}\|$ instead. This approximation is plausible because by (7) all the elements of the matrix $\{\mathcal{E}\}$ are dependent on the unit dynamic errors e_i, $1 \leq i < n$, which constitute the subdiagonal of the matrix, and because $|e_i|$ are greater than $|\mathcal{E}_{i,j}|$ in general.

4 Case Study for Lines

In order to subjectivly verify the use of the dynamic error measure, the special curve, the straight line, which is also the most important graphics primitive, will be examined under this measure. Without loss of generality, it suffices to discuss only lines passing through the origin in the first octant. Suppose that $g(x)$ is such a line, then $y_{i,j} = \lambda(j-i)$, where $\lambda \in [0,1]$ is the slope of the line. Thus on $\mathcal{F}_\circ[g(x)]$ we simply have

$$\mathcal{E}_y = \lambda - Y_{i,j}/(j-i). \tag{20}$$

Since $Y_{i,j}$ equals either $\lfloor y_{i,j} \rfloor$ or $\lceil y_{i,j} \rceil$ constrained by $\mathcal{F}_\circ$, it follows that $\|e\| = 0$ and consequently $\|\mathcal{E}\| = 0$ if and only if $\lambda = 1$ or $\lambda = 0$. In the general case where $\lambda \in (0,1)$, let us assume for simplicity that the line begins and ends at a lattice point such that λ is a rational number P/Q, $0 < P < Q$, where integers P and Q are respectively x and y displacement of the line segment. Then there are P instances of k on $\mathcal{F}_\circ[g(x)]$ such that $Y_{k,k+1} = 1$ and $Q - P$ instances of k' such that $Y_{k',k'+1} = 0$. This fact and (20) lead to

$$\max_{1 \le i,j \le n} \{\mathcal{E}_{i,j}\} = \lambda$$
$$\min_{1 \le i,j \le n} \{\mathcal{E}_{i,j}\} = \lambda - 1, \tag{21}$$

and finally,

$$\|\mathbf{e}\|_\infty = \begin{cases} \max\{\lambda, 1-\lambda\} & 0 < \lambda < 1 \\ 0 & \lambda = 0, 1 \end{cases}. \tag{22}$$

Now consider the 1-norm of $\mathbf{e}$ for an average measurement of the dynamic errors on the discretized lines. There are $Q + 1$ pixels on $\mathcal{F}_\circ[g(x)]$ hence Q unit dynamic errors. Among the e_i, $i = 1, 2, \ldots, Q$, P of them equal $1 - \lambda$ and the rest equal λ. Thus

$$\|\mathbf{e}\|_1 = \sum_{i=1}^{Q} |e_i| = P(1-\lambda) + (Q-P)\lambda. \tag{23}$$

Averaging the total unit dynamic error yields

$$\|\mathbf{e}\|_1/Q = 2\lambda - 2\lambda^2. \tag{24}$$

Figure 3 plots $\|\mathbf{e}\|_\infty$ and $\|\mathbf{e}\|_1/Q$ separately as functions of λ. In Figure 4 there is also visual evidence of the above analytic results in the form of discrete lines with various slopes in the first octant generated by Bresenham's line algorithm. The correspondence between Figures 3 and 4 is convincing. Among all lines in the first octant only the ones with slope of 0 or 1 can be rendered without dynamic error due to the finite precision of raster plane. The others are ap-
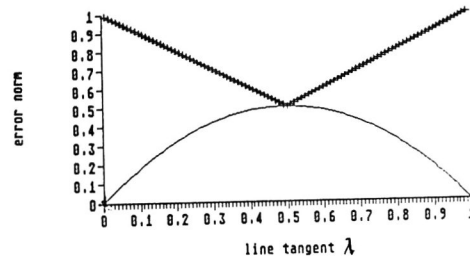

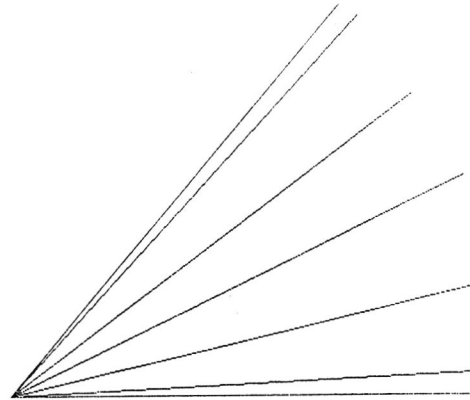Figure 3: Dynamic errors for discrete lines.

Figure 4: Discrete lines generated by Bresenham's algorithm.

proximated by a sequence of horizontal or diagonal straight segments (runs as commonly referred in literature). At the joints of these segments the consistency of the tangent of lines (the sense of the straightness) deteriorates in proportional to λ as shown in Figure 3 (a), with $\|\mathbf{e}\|_\infty$ increasing from 1/2 toward 0 or 1. Under the 1-norm, however, the average dynamic error on a discrete line increases as the slope λ approaches 1/2 from 0 or 1. This is because the closer to 1/2 the slope of a line, the shorter the runs on the discrete line, hence the more runs and more joints of the runs for a given line length, and consequently the larger the total dynamic error. According to the subjective appreciation of the majority of individuals, the discrete lines with slopes near 1/2 are less jaggied than those with slopes closer to 0 and 1. This suggests that all the dynamic errors should be uniformly minimized for a good rendering of the dynamic context of the original curves. The ∞-norm is therefore more appropriate for image quality than the 1-norm.

As a comparison, let us see how well the linear error reflects the difference in image quality for discrete lines of different tangents. The differences are clearly see in Figure

4. Again let the tangent of the line be a rational number P/Q, $0 < P < Q$, and P and Q be relatively prime. The linear error for the lines under discussion is

$$E_i = \frac{P}{Q}i - \left\lfloor \frac{P}{Q}i + 1/2 \right\rfloor. \tag{25}$$

It is easy to verify that

$$
\begin{aligned}
|E_i| &= \left| \frac{P}{Q}i - \left\lfloor \frac{P}{Q}i + 1/2 \right\rfloor \right| \\
&= \min \left\{ \frac{(iP)\,mod\,Q}{Q}, 1 - \frac{(iP)\,mod\,Q}{Q} \right\}. \tag{26}
\end{aligned}
$$

In order to compute $\|\mathbf{E}\|_\infty$ and $\|\mathbf{E}\|_1$, we realize that since P and Q are relatively prime it follows that $(iP)\,mod\,Q \neq (jP)\,mod\,Q$ for $i \neq j$, $1 \leq i, j < Q$, resulting in a one-to-one map from the set $\{(1P)\,mod\,Q, (2P)\,mod\,Q, \ldots, [(Q-1)P]\,mod\,Q\}$ to the set $\{1, 2, \ldots, Q-1\}$. This together with (26) leads to

$$\|\mathbf{E}\|_\infty = \min\left\{ \lfloor Q/2 \rfloor / Q, 1 - \lfloor Q/2 \rfloor / Q \right\} \tag{27}$$

and to

$$
\begin{aligned}
\|\mathbf{E}\|_1 &= \sum_{i=0}^{Q} |E_i| \\
&= \frac{2}{Q} \sum_{i=1}^{\lfloor Q/2 \rfloor} i - \frac{1 - Q\,mod\,2}{2} \\
&= \frac{1 + \lfloor Q/2 \rfloor}{Q} \lfloor Q/2 \rfloor - \frac{1 - Q\,mod\,2}{2}. \tag{28}
\end{aligned}
$$

By (27) and (28) neither $\|\mathbf{E}\|_\infty$ nor $\|\mathbf{E}\|_1$ is dependent on the tangent $\lambda = P/Q$. On the contrary, it is the λ that determines the image quality of the discretized lines as shown in Figure 4. For instance, neither of the measurements $\|\mathbf{E}\|_\infty$ and $\|\mathbf{E}\|_1$ will change for lines of different tangents $1/9$, $2/9$ and $4/9$, while $\|\mathbf{e}\|_\infty$ and $\|\mathbf{e}\|_1$ will vary significantly from one line to the others. Therefore, the linear error E_i is not suitable as a measure for the overall quality of raster images.

It is important to point out that for straight lines $\|\mathcal{E}\|$ depends only on the slopes of lines unlike $\|\mathbf{E}\|$ which is very sensitive to the absolute positions of original lines. For example, from the line $y = x$ to the line $y = x + 1/2$ $\|\mathbf{E}\|_\infty$ jumps from 0 to $1/2$ but $\|\mathcal{E}\|_\infty$ remains 0. This can be explained by the relation between the linear error and the dynamic error $\mathcal{E}_{i,j} = (E_j - E_i)/(j - i)$. The dynamic error was defined to measure the ability of a scan-conversion scheme to preserve the dynamic context of an original curve rather than its static position. Clearly the relative positions between pixels on the discrete images of the two lines are the same, hence the two discrete lines have the same degree of smoothness.

5 Case Study for Convex Curves

For general curves it is difficult to obtain the kinds of closed forms that were obtained for lines. Some conclusions more informative than trivial ones can, however, still be obtained. Suppose that a convex twice differentiable curve $g(x)$ is scan-converted under $\mathcal{F}_0$ from left to right and that the pixels on $\mathcal{F}_0[g(x)]$ are indexed in the same order. Rewrite (6) as

$$\mathcal{E}_{i,j} = \frac{y_{i,j}}{j - i} - \frac{Y_{i,j}}{j - i}. \tag{29}$$

Note that

$$y_{i,i+1} \leq y_{k,k+1} \leq y_{k,k+l}/l, \qquad i \leq k, \ l \geq 2, \tag{30}$$

since $g(x)$ is convex, and note that $0 \leq Y_{i,j} \leq j - i$ since $0 \leq g'(x) \leq 1$ (recall the restriction on the octants made before). Then it follows from (29) and (30) that

$$\min_{1 \leq i,j \leq n} \{\mathcal{E}_{i,j}\} = e_\imath, \tag{31}$$

where $\imath = \min_{1 \leq i < n}\{i | Y_{i,i+1} = 1\}$

Symmetrically, the convexity of $g(x)$ also implies

$$y_{i,i+1} \geq \frac{y_{k,i+1}}{i - k + 1} \geq y_{k,k+1}, \qquad i \geq k. \tag{32}$$

This together with (29) means that

$$\max_{1 \leq i,j \leq n} \{\mathcal{E}_{i,j}\} = e_\jmath, \tag{33}$$

where $\jmath = \max_{1 \leq i < n}\{i | Y_{i,i+1} = 0\}$. Therefore,

$$\|\mathbf{e}\|_\infty = \max\{|e_\imath|, |e_\jmath|\}. \tag{34}$$

The implication of (34) is that the worst dynamic errors are the unit dynamic errors at the the first diagonal pixel move and the last horizontal pixel move if we march counterclockwise along $\mathcal{F}_0[g(x)]$.

Furthermore, by the mean value theorem we get

$$e_i = g'(\xi_i) - Y_{i,i+1}, \tag{35}$$

where $x_i \leq \xi_i \leq x_{i+1}$, and $Y_{i,i+1}$ is either 0 or 1. The above equation subsumes the relation (22) for straight lines. It shows that the dynamic context of curve segments whose tangent is closer to $1/2$ can be better preserved by the scheme $\mathcal{F}_0$ if the criterion is to minimize the maximum magnitude of the dynamic error, i.e., if ∞-norm is adopted.

Now let $\rho_{0,i}$ be the probability that $Y_{i,i+1} = 0$ and $\rho_{1,i}$ be the probability that $Y_{i,i+1} = 1$. It can be qualitatively
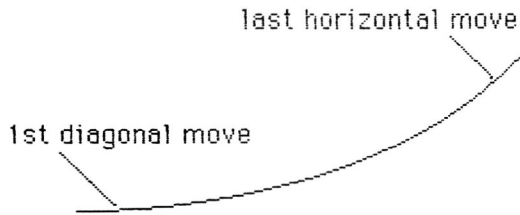
Figure 5: An octant of a discrete ellipse generated by $\mathcal{F}_\diamond$.

said that $\rho_{1,i} \propto g'(\xi_i)$ or, $\rho_{1,i} = cg'(\xi_i)$ and $\rho_{0,i} = 1 - cg'(\xi_i)$ for some $c \in [0,1]$. Thus in term of probability we have

$$
\begin{aligned}
\|\mathbf{e}\|_1 &= \sum_{i=1}^{n-1} |e_i| \\
&= \sum_{i=1}^{n-1} [g'(\xi_i)\rho_{0,i} + [1 - g'(\xi_i)]\rho_{1,i}] \\
&= \sum_{i=1}^{n-1} \left[(1+c)g'(\xi_i) - 2c[g'(\xi_i)]^2 \right]. \quad (36)
\end{aligned}
$$

Clearly, formula (24) is a special case of (36) when $g'(\xi_i) = \lambda$ and $c = 1$. It can be inferred from (36) that compared with the curve segments whose tangents are closer to 0 or 1, the curve segments with their tangents closer to $1/2$ have slightly larger unit dynamic error on the average. In contrast, however, the latter have tighter dynamic error bounds than the former as argued earlier. For the reader's own judgement the raster image of an octant segment of an ellipse generated by $\mathcal{F}_\diamond$ is given in Figure 5. As illustrated in the figure, the ugliest jaggies occur at the two ends of the octant segment verifying (34) and (35). However, the density of the pixel stairs becomes higher from the end to the middle of the octant segment. Hence, as it should be by (36), the average dynamic error is larger at the middle than at the two ends of the segment.

It has been generally agreed that given a curve $g(x)$, $\mathcal{F}_\Box[g(x)]$ is more jaggied than $\mathcal{F}_\diamond[g(x)]$. This subjective opinion is supported by the dynamic error measure. Recall that the dynamic error is defined to be a relative error against the sample distance. Because an $\mathcal{F}_\Box[g(x)]$ is a 4-connected discrete curve, it takes a vertical move at the point where $\mathcal{F}_\diamond[g(x)]$ has a diagonal move, resulting in $|e_i| \to \infty$ due to zero sample distance. Further study is needed for dynamic errors on $\mathcal{F}_\Box[g(x)]$.

6 Conclusions

It has been demonstrated that the proposed dynamic error measure is more objective than the one in current use for raster image quality. The next logical thing to do is, of course, to develop of curve scan-conversion algorithms under the criterion of minimizing the dynamic error so that the most aesthetic raster images can be achieved within the limitation of the diaplay's resolution. This can be posed as an optimization problem of determining the scan-conversion scheme $\mathcal{F}$ catering to a given curve $y = g(x)$ such that the quantity $\|\mathcal{E}\|$ is minimized. Unfortunately, a direct approach to this optimization problem seems to be one of integer programming, being too expensive to be applicable to interactive graphics. Designing more efficient algorithms for optimal curve scan-conversion under the dynamic error measure is still at the research stage.

References

[1] N. I. Badler, *"Disk generations for a raster display device,"*, Computer Graphics and Image Processing, 6, 1977, p. 589-593.

[2] J. E. Bresenham, *"Algorithm for computer control of digital plotting,"* IBM Syst. J. 4, 1965, p. 25-30.

[3] T. J. Ellis, D. Proffitt, D. Rosen, and W. Rutkowski, *"Measurement of the lengths of digitized curved lines,"* Computer Graphics and Image Processing, 10, 1979, p. 333-347.

[4] F. C. A. Groen and P. W. Verbeek, *"Freeman-code probabilities of object boundary quantized contours,"* Computer Graphics and Image Processing, 7, 1978, p. 391-402.

[5] B. K. P. Horn, *"Circle generations for display devices,"*, Computer Graphics and Image Processing, 5, 1976, p. 280-288.

[6] B. W. Jordan, Jr., W. J. Lennon, and B. D. Holm, *"An improved algorithm for the generation of nonparametric curves,"* IEEE Trans. Computer, C-22, 1973, p. 1052-1060.

[7] K. Kishimoto, K. Onaga, and K. Yamamoto, *"Theoretical error assessments of curved line digitization schemes on graphic displays,"* Computer Vision, Graphics, and Image Processing, 35, 1986, p. 170-180.

[8] Z. Kulpa and M. Doros, *"Freeman digitization of integer circles minimizes the radial error,"* Computer Graphics and Image Processing, 17, 1981, p. 181-184.

[9] Z. Kulpa, "*Area and perimeter measurement of blobs in discrete binary pictures*," Computer Graphics and Image Processing, 6, 1977, p. 434-451.

[10] M. D. McIlroy, "*Best approximate circles on integer grids*,", ACM Trans. Graphics, 2, 1983, p. 237-263.

[11] T. Pavlidis, *Algorithms for graphics and image processing*, Computer Science Press, Rockville, MD, 1982.

[12] D. Proffitt and D. Rosen, "*Metrication errors and coding efficiency of chain-encoding schemes for the representation of lines and edges*," Computer Graphics and Image Processing, 10, 1979, p. 318-332.

[13] Y. Suenaga, T. Kamae, and T. Kobayashi, "*A high-speed algorithm for the generation of straight lines and circular arcs*," IEEE Trans. Computer, C-28, 1979, p. 728-736.